

Supporting Information for

Three-Dimensionally Printed Microelectromechanical Switches

Yongwoo Lee^{1,†}, Jungmin Han^{1,†}, Bongsik Choi¹, Jinsu Yoon¹, Jinhee Park¹, Yeamin Kim¹, Jieun Lee¹,
Dae Hwan Kim¹, Dong Myong Kim¹, Meehyun Lim², Min-Ho Kang³, Sungho Kim^{4,*},
and Sung-Jin Choi^{1,*}

¹School of Electrical Engineering, Kookmin University, Seoul 02707, Korea

²Mechatronics R&D Center, Samsung Electronics, Gyeonggi-do 18448, Korea

³Department of Nano-process, National Nanofab Center (NNFC), Daejeon 34141, Korea

⁴Department of Electrical Engineering, Sejong University, Seoul 05006, Korea

Email: sjchoiee@kookmin.ac.kr and sungho85kim@sejong.ac.kr

[†]These authors equally contributed to this work.

S1. Main components of the FDM-based 3D printer

Figure S1 shows photographic images of the 3D printer, which operates based on the FDM method, and the main components of the 3D printer, including the bed, fans, and extruder. Thermoplastic material is printed on the bed at a controlled temperature. The bed can move semi-automatically in the vertical direction, and care must be taken to properly adjust the printing position. A fan is located on each side of the extruder to cool the printed thermoplastic to quickly to solidify it. As a component of the extruder, the heating coil melts the thermoplastic by heating it to a temperature exceeding its melting point. As another component of the extruder, the nozzle can withstand temperatures exceeding the melting points of 3D-printable thermoplastics, as it is composed of stainless steel with low thermal conductivity.

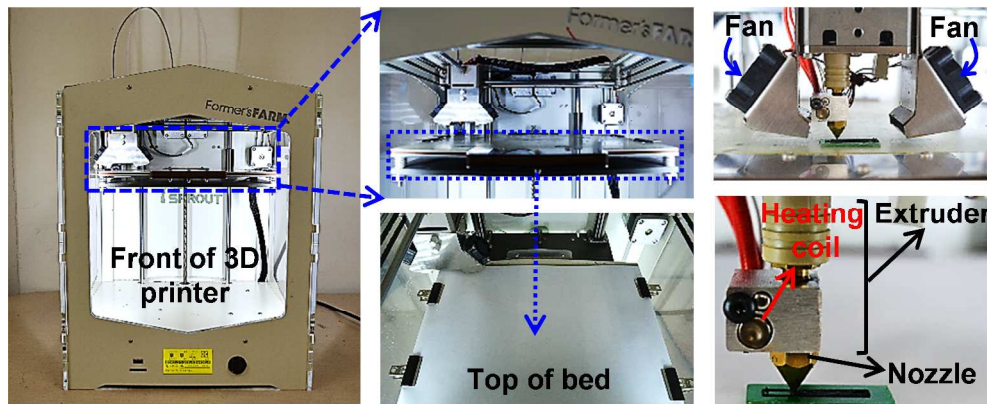


Figure S1. Photographs of the FDM-based 3D printer used to fabricate the 3D-printed MEM switches and its components.

S2. Top-view micrograph images of the 3D-printed CPLA of various densities

Figure S2 shows top-view micrograph images of the 3D-printed CPLA layers of various densities (25%, 50%, 75%, and 100%). The internal density of the printed structures can easily be controlled using a 3D printer; hence, a higher density can generate enhanced surface properties in the printed structures. As the two electrodes are in contact with one another in an on state in our 3D-printed MEM switches, it is necessary to print the CPLA at a density of 100% to improve surface characteristics.

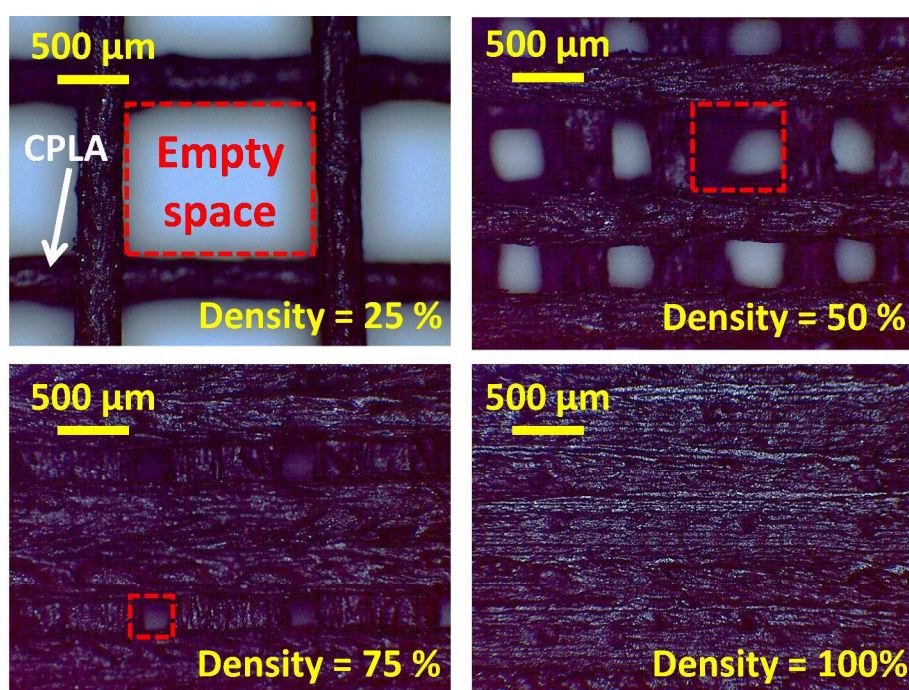


Figure S2. Micrograph images of the 3D-printed CPLA layers of various densities (25%, 50%, 75%, and 100%).

S3. Derivations of the k_{eff} equation and calculations of the normalized k_{eff} values for the two-terminal MEM switches

In our previous study, the k_{eff} for two-terminal MEM switches with a hammerhead structure is denoted by the following equation:

$$k_{eff} = \frac{24EI_m y}{3(L_{se} - x)(L_{se} + x)^2 + 2yx^2(x + 3L_{se}) + 12xL_{se}(L_{se} - x)(y - 1)} \quad (S1)$$

where I_m is the moment of inertia of the suspended electrode and y is a constant value that divides the W_2 of 4.1 mm by the W_1 of 0.8 mm. Here, I_m is defined by solving the following:

$$I_m = \frac{W_1 t_{se}^3}{12} \quad (S2)$$

Therefore, by rearranging the y value (5.125) and by adding Eq. S2 to Eq S1, the modified k_{eff} equation can be expressed.

Moreover, to investigate the effect of x on k_{eff} , we calculated normalized k_{eff} values as a function of x . Figure S3a presents a schematic illustration of MEM switches with increasing x values; Figure S3b shows the normalized k_{eff} results. As x increases, k_{eff} ultimately reaches a negative value. The k_{eff} values were normalized with respect to the value corresponding to $x = 0$.

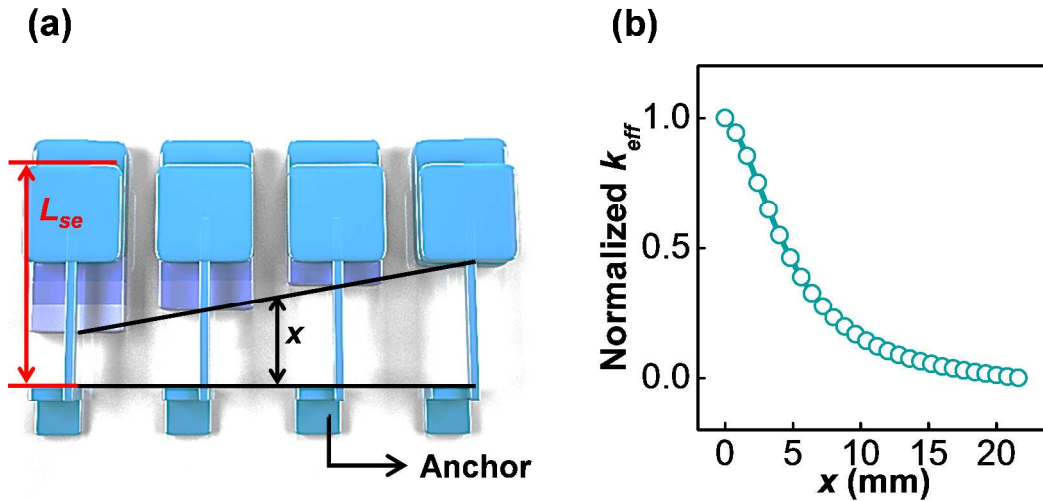


Figure S3. (a) Schematic illustration of 3D-printed MEM switches with increasing x values. (b) Calculated normalized k_{eff} values for different x values.

S4. Calculation of the Young's modulus for the 3D-printed CPLA

To examine the mechanical properties of the printed CPLA, we measured the Young's modulus (E) of several CPLA samples using the American standard test method (ASTM) D638. Samples of a predetermined standard size were printed, and E was then measured for each sample by analysing the measured stress relative to the applied strain at a strain rate of 9.75 mm/sec as shown in Figure S4a. The value of E can be extracted from the initial slope of the stress-strain curve and thus it can be expressed as the following equation:

$$E = \left. \frac{d(stress)}{d(\Delta L/L_0)} \right|_{\Delta L/L_0=0} \quad (S3)$$

where L_0 is the initial length of the sample and ΔL is the stretched length of the sample. We measured the stress-strain curves of six CPLA samples. The average E value of the samples was found to be approximately $2465 \text{ MPa} \pm 500 \text{ MPa}$ as shown in Figure S4b and Figure S4c. Notably, we printed the CPLA 100% density when fabricating the 3D-printed MEM switches; however, CPLA density can be controlled during 3D printing, suggesting that the E value can be adjusted by varying the density level. This density dependence of the mechanical properties of 3D-printed materials is expected to afford 3D-printed MEM switches additional design versatility; density levels can be adjusted to tune E , which in turn determines the k_{eff} value of the suspended CPLA electrode.

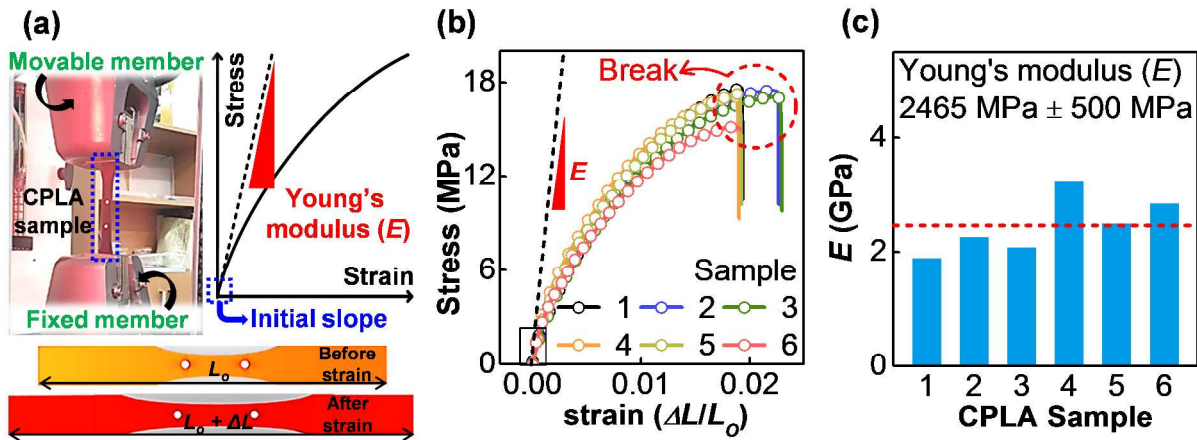


Figure S4. (a) Procedure for measuring E values of the printed CPLA samples. The values of E were extracted from the measured stress-strain curves. (b) The stress-strain curves from which the E values were extracted. (c) The E values extracted from the six samples.

S5. Selectivity and volume change of the sacrificial PVA layer in water

To confirm the selectivity and volume change behaviours of the PVA in DI water, we immersed a 3D-printed PVA layer printed on a CPLA layer with dimensions of $10\text{ mm} \times 10\text{ mm} \times 0.5\text{ mm}$ in DI water. As shown in Figure S5a, the printed PVA layer dissolved fully within a few minutes. After dissolving the PVA layer in DI water, we found no deformation of or damage to the CPLA. No significant volume changes were observed when comparing volumes of the CPLA before and after PVA dissolution, as shown in Figure S5b.

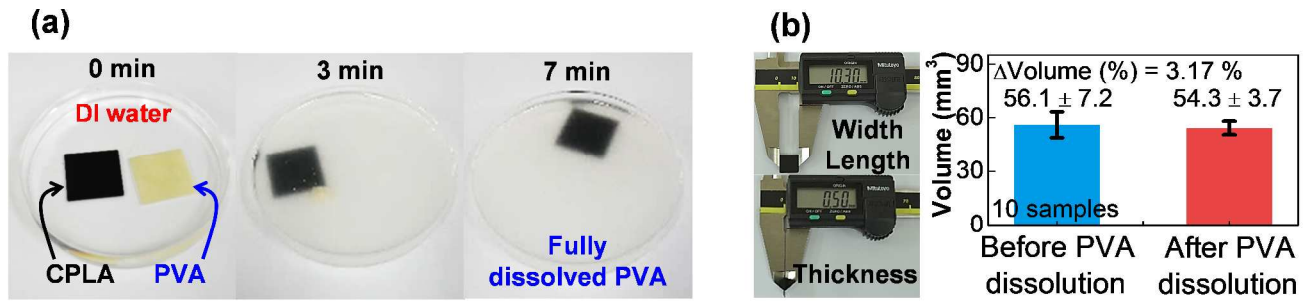


Figure S5. (a) Dissolution of a 3D-printed PVA layer in DI water. (b) Volume change of the CPLA sample before and after PVA dissolution.

S6. Measurement of the resistivity of CPLA using the Van der Pauw method.

To investigate the electrical properties of CPLA, we measured CPLA resistivity using the Van der Pauw method. The Van der Pauw method can be used to accurately measure the characteristics of any arbitrary shape so long as the sample is approximately two-dimensional and solid and has electrodes in place. First, one can flow the current along one edge of the sample and measure the voltage across the opposite edge. Further, by changing the direction of the current and by measuring the voltage, two voltage drop values can be obtained. By measuring the voltage by shifting the electrode in the clockwise direction as shown in Figure S6a, the electrical resistivity (ρ) of CPLA can be derived from a total of eight voltage drop values. ρ is expressed by the following equation:^{S1}

$$\rho_A = \frac{\pi}{\ln 2} f_A t_{CPLA} \frac{(V_1 - V_2 + V_3 - V_4)}{4I} \quad (S4)$$

$$\rho_B = \frac{\pi}{\ln 2} f_B t_{CPLA} \frac{(V_5 - V_6 + V_7 - V_8)}{4I} \quad (S5)$$

$$\rho = \frac{\rho_A + \rho_B}{2} \quad (S6)$$

where f_A and f_B are geometric factors based on sample symmetry, t_{CPLA} is the thickness of the CPLA sample, $V_1 - V_8$ denote measured voltages, and I is the current injected through the CPLA sample. f_A and f_B can be extracted from Eq. S7 and Eq. S8, respectively, as follows:

$$\frac{Q_A - 1}{Q_A + 1} = \frac{f_A}{\ln 2} \operatorname{arccosh} \left(\frac{e^{\ln 2 / f_A}}{2} \right) \quad (S7)$$

$$\frac{Q_B - 1}{Q_B + 1} = \frac{f_B}{\ln 2} \operatorname{arccosh} \left(\frac{e^{\ln 2 / f_B}}{2} \right) \quad (S8)$$

where Q_A and Q_B are the ratio of the resistance measured from the length and width directions of the CPLA sample. Q_A and Q_B are calculated as follows:

$$Q_A = \frac{V_1 - V_2}{V_3 - V_4} \quad (S9)$$

$$Q_B = \frac{V_5 - V_6}{V_8 - V_7} \quad (\text{S10})$$

We calculate Q_A and Q_B from Eq. S9 and Eq. S10, respectively, with the measured voltage values and substitute them into Eq. S7 and Eq. S8 to derive f_A and f_B values by numerical calculation. Finally, we obtain ρ_A and ρ_B from Eq. S4 and Eq. S5 and we determine the ρ value for CPLA from Eq. S6.

Our printed CPLA sample size is 10 mm \times 10 mm \times 0.5 mm and the actual measurement image is shown in Figure S6b. We confirm that printing and dissolving the sacrificial PVA layer did not significantly affect the ρ of CPLA by measuring ρ from the test thin-plate-like printed CPLA using the Van der Pauw method as shown in Figure S6c.

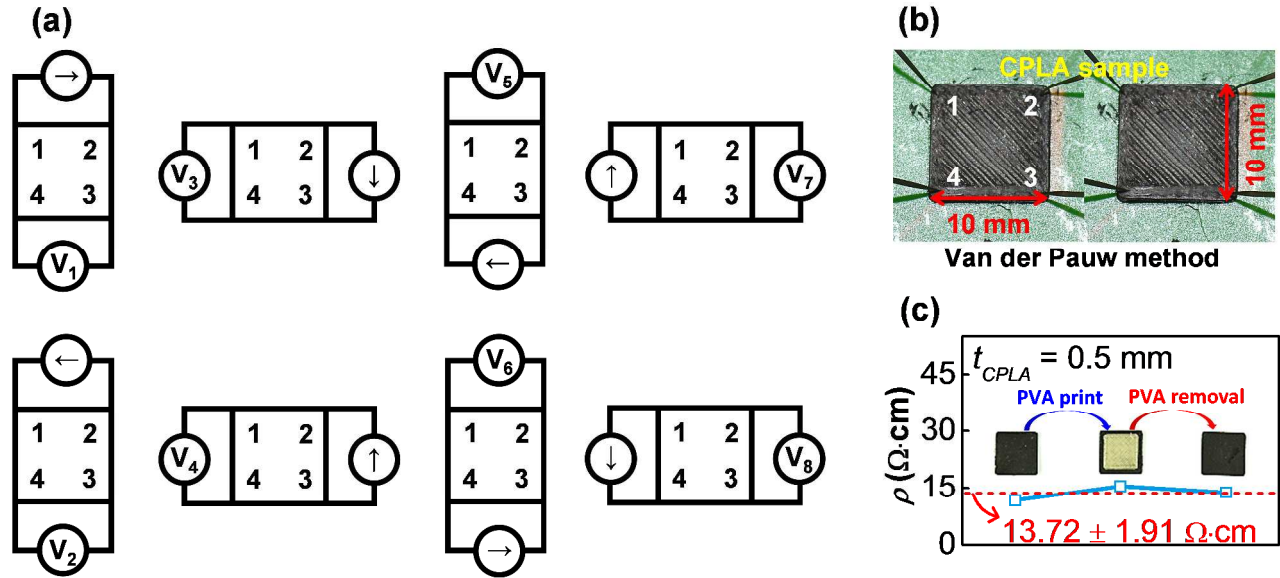


Figure S6. (a) The sequence of Van der Pauw method measurement procedures. (b) Images of the CPLA samples for measuring ρ via the Van der Pauw method. (c) ρ values extracted from printed CPLA, from CPLA after PVA printing on the CPLA, and from CPLA after the removal of PVA samples.

REFERENCES

- (S1) Ramadan, A. A.; Gould, R. D., Ashour, A. A. On the Van Der Pauw Method of Resistivity Measurements. *Thin Solid Films* **1994**, 239, 272-275.